JOURNAL OF APPLIED ELECTROCHEMISTRY 16 (1986) 867–874

Phase composition and structure of silver–antimony alloy deposits plated from ferrocyanide–thiocyanate electrolytes

I. KRISTEV, M. NIKOLOVA

Institute of Physical Chemistry, Bulgarian Academy of Sciences, 1040 Sofia, Bulgaria

Received 19 August 1985; revised 29 October 1985

The structure and phase composition of silver–antimony alloy deposits plated from ferrocyanide–thiocyanate electrolytes is investigated. It is shown that the co-deposition of antimony leads to an abrupt decrease of twinning and the formation of perfect orientation of the crystallites in the alloy along the axis ⟨1 1 1⟩. The co-deposition of antimony exerts a depolarization effect upon the plating process of the alloy. At higher antimony concentrations in the electrolyte and higher deposition current both ζ-phase and ε-phase of the silver–antimony alloy may be formed as well as the pure antimony phase. The concentration regions of antimony in the alloy, within which the different phases are formed and exist, are in agreement with the requirements of the phase diagram. The separate antimony phase is formed at lower antimony concentrations in the alloy than indicated by the phase diagram. The co-deposition of antimony leads to an increase of the crystal lattice parameter of silver and a substantial augmentation of the hardness of the deposited layers.

1. Introduction

The alloying of silver with other elements is practised in order to achieve increased hardness and wear-resistance of the deposits, higher stability against tarnishing, improved antifriction properties, etc. In most cases, when the deposits are designed for use by the electrical engineering and electronic industries, the content of alloying elements is restricted within the range of several percent since as a general rule alloying reduces the electroconductivity of silver. In such cases a compromise between the physico-mechanical and electrical parameters of the deposit is sought.

The silver–antimony alloy has been known for many years. It has been used as an electroplated deposit because of its increased hardness and wear-resistance, which in turn leads to the use of smaller plate thickness and consequent savings of the expensive metal.

According to the phase diagram of the silver–antimony system [1], four phases can emerge in the alloy. The first α-phase represents f.c.c. silver lattice expanded by the antimony atoms substituting some of the silver atoms. It is stable up to an antimony content of 6–7 at % in the alloy. At higher contents of antimony the ζ-phase is formed, which is stable within the antimony content range 8.6–15.6 at %, has a hexagonal lattice and approximate composition Ag_8Sb_1. The next phase of the silver–antimony system is the ε-phase, which, according to the phase diagram, exists within the concentration range 19.1–26.6 at % antimony and is characterized by an orthorhombic lattice and approximate composition Ag_3Sb_1. At an antimony content in the alloy of above 27 at % a pure antimony phase may be formed. From the phase diagram of this system it becomes clear that deposits of practical interest must comprise the α-phase in order to meet electrical requirements. The increase of antimony content in the alloy leading to the formation of the other phases would substantially decrease electroconductivity since antimony has a conductivity only 3.6% of that of silver [2].

The electrodeposition of silver–antimony alloys is carried out mainly in cyanide electrolytes, both in the presence or absence of organic

0021-891X/86 $03.00 + .12 © 1986 Chapman and Hall Ltd.

additives [3–15]. Silver–antimony electrodeposits plated from cyanide electrolytes [4] contain the α-phase of the alloy, but the authors suggest that 'due to uncontrollable changes in the electrodeposition conditions, the appearance of any of the other phases of the alloy is not excluded'.

Taking into consideration the toxicity of cyanide baths, several attempts have been made to plate the alloy from other electrolytes, e.g. ferrocyanide [16–19], thiosulphate [20], succinimide [21], etc. One of the most likely possibilities for the replacement of the cyanide electrolytes for the electrodeposition of silver–antimony alloys is the ferrocyanide bath, containing thiocyante as an anodic depassivator. The introduction of antimony in a similar electrolyte is possible by using potassium antimonyl tartrate [16–19].

The present investigation is aimed at the study of the structure of silver–antimony alloys electrodeposited from ferrocyanide–thiocyanate electrolytes and the determination of their phase composition.

2. Experimental details

The basic electrolyte used in these studies contained the following components (in $g l^{-1}$): $AgNO_3$, 25; $K_4Fe(CN)_6 \cdot 3H_2O$, 70; K_2CO_3, 30; KSCN, 150; $KNaC_4H_4O_6 \cdot 4H_2O$, 60; $KSbOC_4H_4O_6 \cdot \frac{1}{2}H_2O$ at amounts corresponding to 2.5, 5 and 10 $g l^{-1}$ antimony in the electrolyte. The substrates were copper plates, 4 cm^2 in area, with a wire framework. A cell of volume 100 cm^3 was used. Deposition was under galvanostatic conditions with varied cathodic current density (CD) within the range 0.1–2 A dm^{-2}. The polarization curves were also traced under galvanostatic conditions, each point corresponding to a separate test sample. A platinum wire spiral, silver plated (at a CD of 0.5 A dm^{-2} for 30 min) in the above-mentioned electrolyte, containing no antimony, was used as a reference electrode in conjunction with a Luggin capillary. The thickness of the alloy deposits was 20 μm. The percentage of antimony in the deposits (G_{Sb}) was determined by volumetric analysis. Samples designed for the determination of G_{Sb} were plated onto platinum substrates with the same configuration as the copper ones.

3. Results and discussion

When an antimony-containing salt, in our case potassium antimonyl tartrate, is added to electrolyte No. 1, used in a previous paper [22], it is possible to plate silver–antimony alloy deposits. The Seignette salt ($KNaC_4H_4O_6 \cdot 4H_2O$) in the formulation of the electrolyte serves as a supplementary stabilizer of the antimony complex. The addition of antimony to

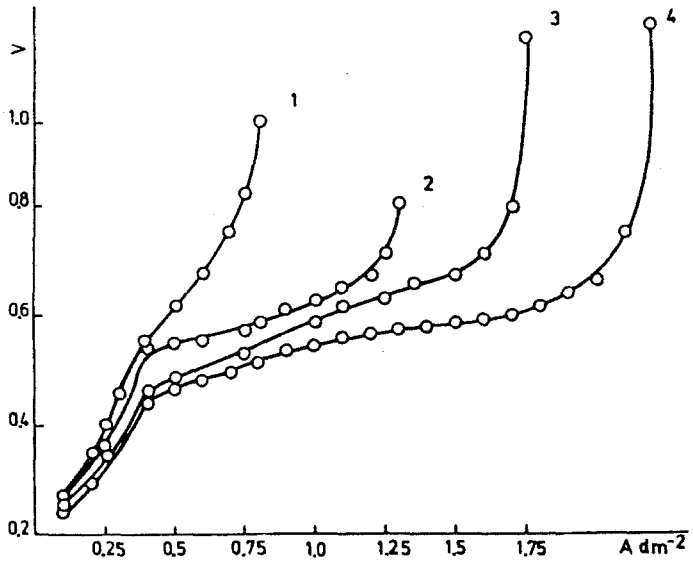

Fig. 1. Electrode potential versus CD. Curve 1, basic electrolyte without antimony; curve 2, 2.5 $g l^{-1}$; curve 3, 5 $g l^{-1}$; curve 4, 10 $g l^{-1}$.

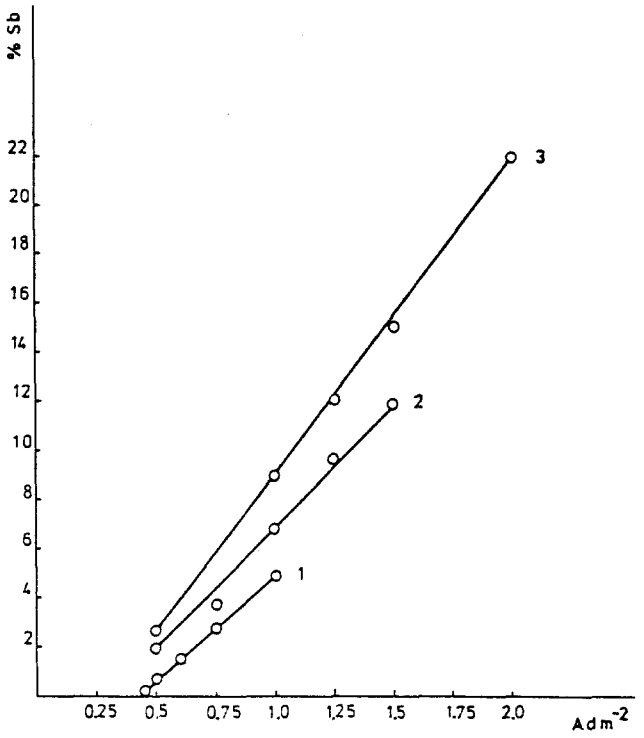

Fig. 2. Antimony content of the alloy versus cathodic CD. Curve 1, 2.5 g l^{-1}; curve 2, 5 g l^{-1}; curve 3, 10 g l^{-1} antimony in the electrolyte.

the basic electrolyte exerts a depolarizing effect upon the deposition of the alloy. This can be seen in Fig. 1, presenting the relationship between cathodic potential and CD. Each point of these curves is a separate sample, since the consecutive tracing of all points using the same sample creates difficulties due to the alteration of the alloy composition at each CD.

The depolarization effect of antimony during the co-deposition with silver is in agreement with data reported by other authors [23] who investigated the deposition of the alloy from cyanide electrolytes. Obviously a similarity exists in the behaviour of silver plating electrolytes based on cyano–argentate complexes even when alloys are plated (compare with [22]).

According to literature data the G_{Sb} of alloy deposits plated from cyanide electrolytes depends on the cathodic CD, bath temperature, agitation and the concentration of antimony in the electrolyte (C_{Sb}). The known relationship between G_{Sb} and CD has a linear character [5, 15]. The increase of temperature and agitation of the bath decreases the antimony content in the deposit, while a higher antimony concentration in the electrolyte exerts a reverse effect.

The antimony content of the alloy deposits is shown in Fig. 2. The deposits were plated without agitation of the electrolyte at 20° C on a platinum substrate. The figure shows clearly that at $C_{Sb} = 2.5\,g\,l^{-1}$ and CD $\sim 0.4\,A\,dm^{-2}$ no antimony is detected in the deposit, i.e. at potentials up to about 540 mV only pure silver is plated. At a C_{Sb} of 5 g l^{-1} no antimony is co-deposited up to 0.3 A dm^{-2}, i.e. approximately 400 mV. Within the investigated CD range the curves display a linear character.

The comparison of Figs 1 and 2 shows that at low cathodic CDs when no antimony is co-deposited, the polarization curves are situated close to each other. The co-deposition of antimony is related to a change in the shape of curves 2 to 4 as compared with curve 1, i.e. the depolarization effect is observed in the region where antimony co-deposition occurs.

The investigation of deposits plated from electrolytes containing no antimony have shown [22] that the main orientation of the crystallites in the deposit is ⟨1 1 1⟩ acompanied by orientation along ⟨3 1 1⟩ and twinning along ⟨5 1 1⟩, and when CD is increased the textured component ⟨3 1 1⟩ decreases and a transition from

⟨1 1 1⟩ and ⟨5 1 1⟩ to random deposits is observed.

During the co-deposition of antimony the picture is somewhat similar to phenomena observed in the case of pure silver plating. At low CD the texture is ⟨1 1 1⟩ + ⟨5 1 1⟩ together with ⟨3 1 1⟩. As the CD increases, the orientation ⟨3 1 1⟩ also disappears and within the antimony co-deposition region a substantial decrease of ⟨5 1 1⟩ twins is observed, and the orientation is purely along the axis ⟨1 1 1⟩. At $C_{Sb} = 2.5\,g\,l^{-1}$ and CDs above $1\,A\,dm^{-2}$ where the deposits are of no practical interest, this orientation reduces its perfection and finally random orientation is again reached. At concentrations of $5\,g\,l^{-1}$ the picture is similar. The ⟨3 1 1⟩ orientation is observed up to $0.25\,A\,dm^{-2}$. Orientations ⟨1 1 1⟩ and ⟨5 1 1⟩ are observed up to $0.75\,A\,dm^{-2}$, while at $1–1.25\,A\,dm^{-2}$ a ⟨1 1 1⟩ orientation with no twinning is observed. At CDs higher than $1.5\,A\,dm^{-2}$ the deposits are random oriented.

At an antimony concentration of $10\,g\,l^{-1}$ the orientation ⟨3 1 1⟩ also exists up to $0.25\,A\,dm^{-2}$. Between 0.5 and $1\,A\,dm^{-2}$ a pure ⟨1 1 1⟩ orientation is obtained, which at higher CDs decreases its perfection and after a transition to random oriented deposits, at approximately $1.5\,A\,dm^{-2}$, again shows X-ray peaks. These maybe attributed to the hexagonal phase and would correspond to a mixed texture along the axes ⟨0 0 0 1⟩ and ⟨1 0 $\bar{1}$ 0⟩ but with a very poor perfection. At $2\,A\,dm^{-2}$ the deposits display random orientation.

These results differ from those obtained in the absence of antimony by the observed phenomenon that within the CD range $0.75–1.2\,A\,dm^{-2}$ at $C_{Sb} = 2.5\,g\,l^{-1}$, as well at $0.5–1.25\,A\,dm^{-2}$ at $5\,g\,l^{-1}$, or $0.5–1.0\,A\,dm^{-2}$ at $10\,g\,l^{-1}$, a pure orientation without twinning is obtained. The latter is observed within the antimony content range in the deposit 3–6 wt % at $2.5\,g\,l^{-1}$, 2–9 wt % at $5\,g\,l^{-1}$ and 2.7–9.0 wt % at $10\,g\,l^{-1}$ antimony in the electrolyte.

The co-deposition of antimony affects the lattice parameter of silver. Raub *et al.* [4] have shown that the silver lattice parameter is increased as the concentration of antimony in the alloy plated from cyanide electrolytes is increased. Our X-ray diffraction investigations also suggest that the increase of G_{Sb} leads to an augmentation in the silver lattice parameter.

Fig. 3 shows the relationship between the silver lattice parameter and the percentage of antimony in the alloy (G_{Sb}) for the three investigated values of C_{Sb}. The silver lattice parameter increases up to approximately 4.12 Å and a plateau appears further on. Literature data suggest that in the case of metallurgical alloys the silver lattice can expand under the effect of antimony up to a lattice parameter of 4.116 Å [24]. It is quite logical to presume that from this moment on, antimony co-deposition should follow a different pattern, i.e. it may be possible to deposit the next silver–antimony alloy phase. However, it turned out that the three curves do not coincide, i.e. the plateau of the lattice parameter starts at different antimony concentrations in the lattice. Raub *et al.* [4] claim that the saturation limit of the α-phase in electrodeposited alloys is within the region 3.6–7.0 at % antimony. The curves for alloys plated in 2.5 and $5\,g\,l^{-1}$ antimony-containing electrolytes are approximately within this antimony content range. At $10\,g\,l^{-1}$ antimony, however, the plateau of the curve is reached at

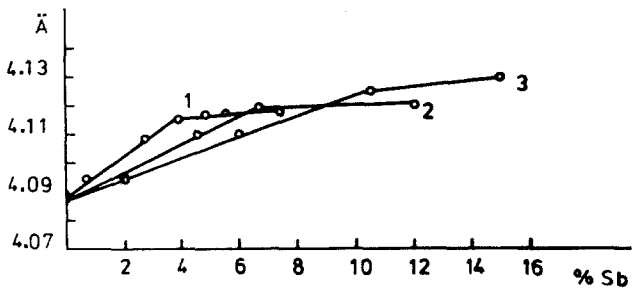

Fig. 3. Crystal lattice parameter of silver versus antimony content in the deposit. Concentration of antimony in electrolyte: curve 1, $2.5\,g\,l^{-1}$; curve 2, $5\,g\,l^{-1}$; curve 3, $10\,g\,l^{-1}$.

approximately 10 wt % antimony in the alloy. Here we must take into consideration that different curves with identical antimony content percentages are traced under different electrochemical conditions. At high C_{Sb} the other phases of the alloy are also formed as well as the pure antimony phase. Therefore, only part of the deposited antimony corresponds to the α-phase whose lattice parameter is measured, so that curves 2 and 3 must shift towards curve 1. Under the conditions of curve 1, i.e. 2.5 g l^{-1} antimony in the electrolyte, no peaks corresponding to another phase are seen on the X-ray diffraction patterns. Nevertheless, if such a phase is formed, some indirect evidence should be available. It must be noted at this point that the deposits are strongly textured. Considering the perfect texture along the ⟨1 1 1⟩ axis of the f.c.c. α-phase under these conditions and the similarity in the structure of the (1 1 1) planes of the f.c.c. lattice and (0 0 1) planes of the hexagonal lattice, it could be presumed that an eventual hexagonal phase is oriented along the ⟨0 0 0 1⟩ axis. In this case it would have interplanar distances (0 0 0 2) such that the diffraction peaks corresponding to f.c.c. (1 1 1) and hexagonal (0 0 0 2) will partially overlap and the two phases will become virtually indistinguishable. The absence of twinning within this range could be regarded as indirect evidence for the existence of a hexagonal phase. However, if we take into consideration the low antimony contents in the alloy deposited from electrolytes containing 2.5 g l^{-1} antimony, we must direct our search for the next phase at higher antimony content in the alloy, i.e. plated from high antimony baths.

Fig. 4 shows a set of diffraction patterns of samples deposited at different CDs and containing various amounts of antimony at C_{Sb} = 5 g l^{-1}, traced with a Co$K\alpha$ radiation tube. This figure shows that with increase of CD leading to an increase of G_{Sb} the reflections of the lines {2 0 0}, {2 2 0} and {3 1 1} abruptly decrease their intensities and finally disappear, i.e. the orientation along the ⟨1 1 1⟩ axis is enhanced as already mentioned when textures were discussed. At CDs within the range 1.25–1.5 A dm^{-2} at small angles, 2θ, a slight enhancement of the background of the diffraction patterns is observed, reflecting an amorphous portion of

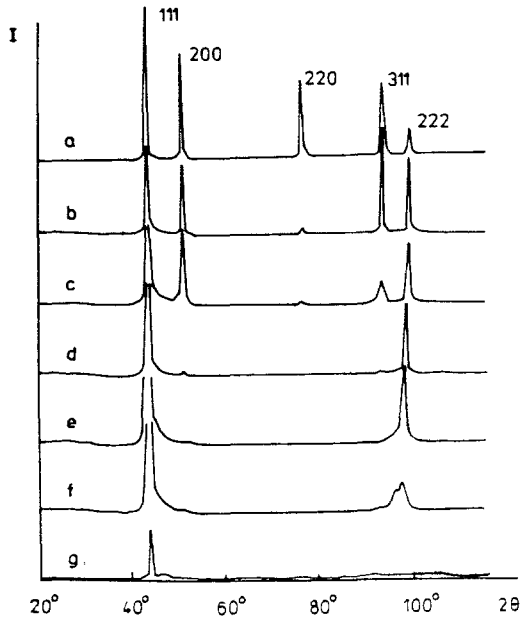

Fig. 4. Diffraction patterns (Co$K\alpha$ radiation) of deposits plated at different current densities from electrolyte containing 5 g l^{-1} antimony. a, 1 A dm^{-2}, no antimony in the electrolyte (blank test); b, 0.25 A dm^{-2}; c, 0.5 A dm^{-2}; d, 0.75 A dm^{-2}; e, 1 A dm^{-2}; f, 1.25 A dm^{-2}; g, 1.5 A dm^{-2}.

the deposit. At CDs above 1.5 A dm^{-2} a general decrease of the intensity of the diffracted rays is registered; also there is evidence for the presence of an increased amorphous deposit. In this case the deposits are dark grey to black and are spongy. A splitting of the {2 2 2} peak is observed in the CD interval 1.25–1.5 A dm^{-2} while the {1 1 1} peak shows an increase in its width, and it also splits only when the CD exceeds 1.5 A dm^{-2}. These two peaks correspond to the reflections (1 0 0) and (1 1 2) of the hexagonal phase. Consequently we may claim that the ζ-phase in this case is observed with intrinsic peaks starting from CDs of 1.25 A dm^{-2}, i.e. about 9.5 wt % antimony in the alloy.

Fig. 5 shows several typical diffraction patterns traced with Cu$K\alpha$ radiation at different CDs and C_{Sb} = 10 g l^{-1}. In this case the changes in the phase composition are observed more easily due to the increased amounts of antimony in the alloy. Similarly to the case with C_{Sb} = 5 g l^{-1}, as the amount of antimony in the alloy increases the {2 0 0}, {2 2 0} and {3 1 1} reflections disappear, the ⟨1 1 1⟩ texture becomes more perfect, and at a CD of 1 A dm^{-2} (9 wt % antimony

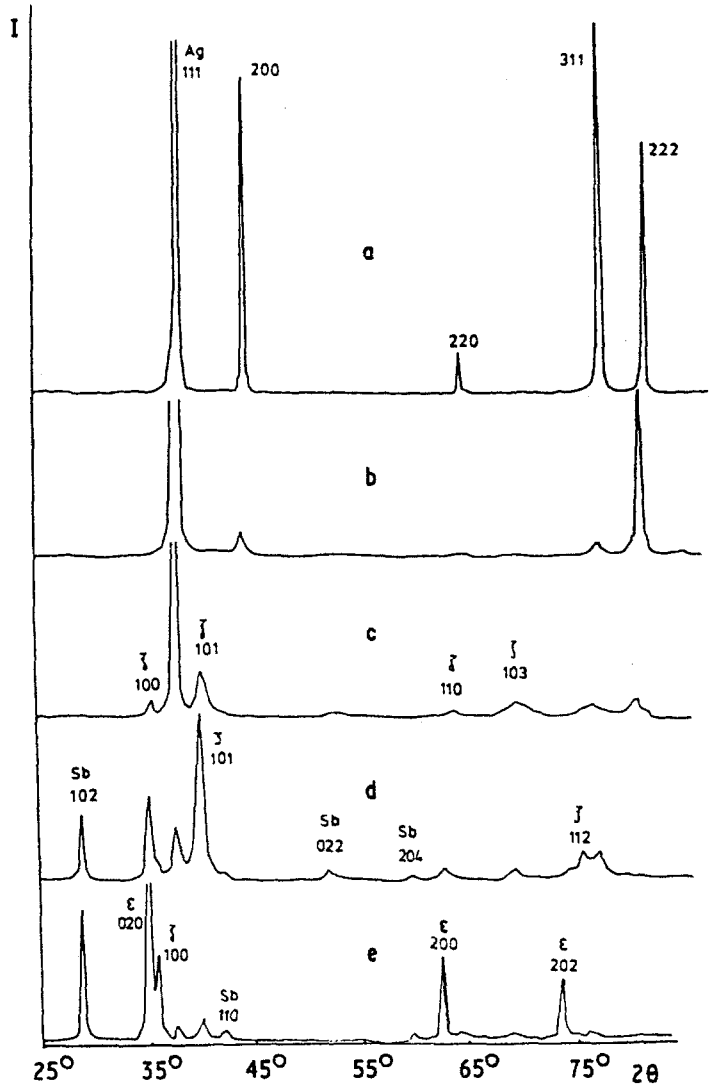

Fig. 5. Diffraction patterns (Cu$K\alpha$ radiation) of deposits plated from electrolyte containing 10 g l^{-1} antimony. Values of CD: a, 0.25 A dm^{-2}; b, 0.75 A dm^{-2}; c, 1.5 A dm^{-2}; d, 1.75 A dm^{-2}; e, 1.9 A dm^{-2}.

in the alloy) the peaks of the hexagonal phase can be observed. At higher G_{Sb} the α-phase peak decreases and those of the hexagonal phase are increased, while a separate pure antimony phase peak appears starting from 14–15 wt % antimony in the alloy. At 19 wt % antimony the ε-phase begins to appear, clearly visible in the last diffraction pattern where the peaks of this phase dominate all other peaks.

Consequently, these investigations show that all phases of the silver–antimony system, as well as pure antimony, can be formed in the alloys studied. We can also determine the limits for formation of each phase on the basis of the respective peaks. The fact that a pure antimony phase is observed at G_{Sb} lower than 27%, in agreement with data reported by Fedotjev and Vjacheslavov [25] in the case of cyanide electrolytes, is very impressive. The presence of free antimony in the alloy could serve as an indirect explanation of the divergence of the curves in Fig. 3. Fig. 6 shows the CDs, the values of G_{Sb} and the corresponding textures and phases obtained under these conditions.

The limits of appearance and existence of the different phases are generally in agreement with the phase diagram of the system. The only exception is pure antimony appearing as a phase at lower concentrations in the alloy.

Fig. 7 presents the microhardness of the

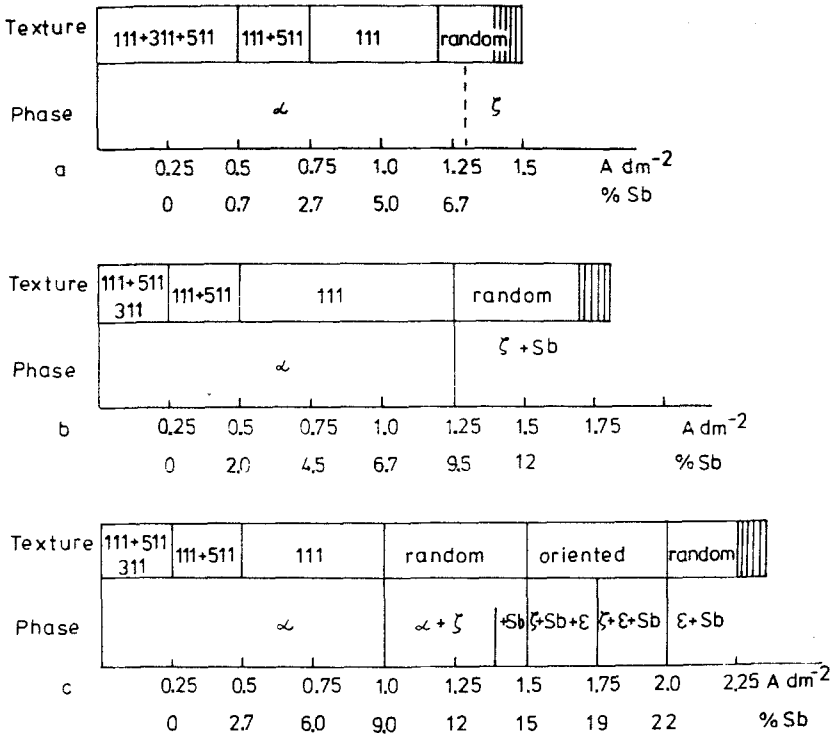

Fig. 6. Textures and phases formed during the deposition of silver–antimony alloys with the following antimony concentrations in the electrolyte: a, 2.5 g l^{-1}; b, 5 g l^{-1}; c, 10 g l^{-1}.

deposits plotted versus the percentage of antimony in the alloy deposit. For all three values of C_{Sb} the points fit a curve which reaches a plateau at approximately 2–3 wt % antimony in the alloy, i.e. contents which are the maximum admissible for practical applications of the alloy. Literature data [19] claim that maximum wear resistance is obtained at these antimony contents, i.e. up to 15 times that of pure silver. Therefore plating electrolytes containing 5 g l^{-1} antimony and operating at 0.5 A dm^{-2} may find practical applications.

4. Conclusions

1. It has been established that the co-deposition of antimony with silver from ferrocyanide–thiocyanate electrolytes exerts a depolarization effect.

2. The relationship between the percentage of antimony in the alloy and cathodic CD is linear.

3. The textures of the silver–antimony alloys are similar to those of pure silver deposited in the same basic electrolyte and, within the region of maximum expansion of the silver crystal lattice, the twinning orientation ⟨5 1 1⟩ disappears and a pure ⟨1 1 1⟩ orientation is obtained. At high CDs a transition from pure ⟨1 1 1⟩ to random orientation occurs.

4. It is shown that from ferrocyanide–thiocyanate electrolytes with high antimony concentrations and at elevated CDs, not only the α-phase of the alloy can be plated but also the ζ- and ε-phases as well as pure antimony. The regions where the different phases appear are in agreement with the phase diagram of the alloy, with the exception of the pure antimony phase which is found at substantially lower antimony contents in the alloy.

5. It is possible that formation of a following phase commences before the previous one has been saturated with antimony.

6. The co-deposition of small amounts of antimony leads to an abrupt increase of microhardness of the coatings.

7. The alloy can find practical applications

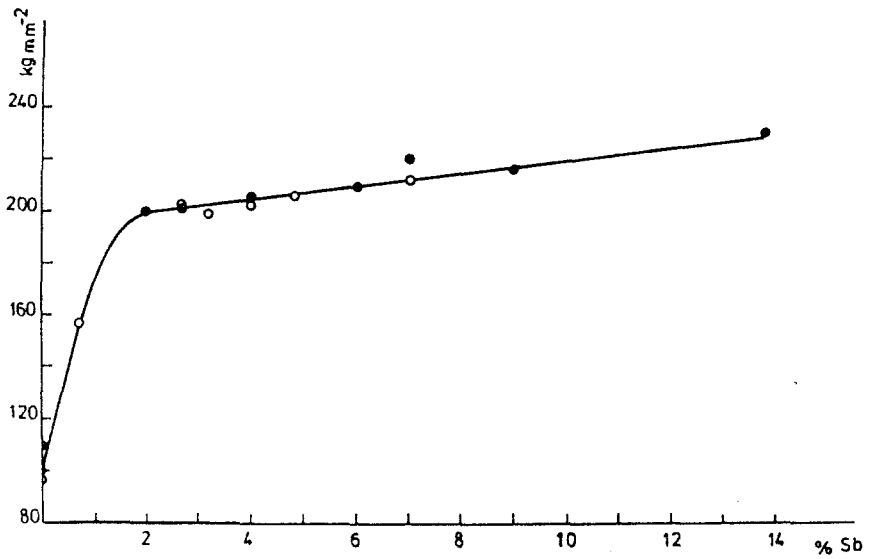

Fig. 7. Microhardness of the deposits versus antimony content in the alloy plated in different electrolytes, containing the following concentrations of antimony in the electrolyte: 2.5 $g l^{-1}$; 5 $g l^{-1}$; 10 $g l^{-1}$.

provided deposition is carried out under conditions leading to the formation of the α-phase.

References

[1] M. Hansen and K. Anderko, 'Srukturi dvojnih splavov', Metallurgizdat, Moscow, Vol. 1 (1962) p. 63 (in Russian).
[2] H. Remy, 'Lehrbuch der anorganischen Chemie', Akad. Verlagsgesellschaft Geest & Portig K. G., Leipzig, Bd. I, (1960) p. 780.
[3] A. Brenner, 'Electrodeposition of Alloys', Vol. 1, Academic Press, New York and London (1963) p. 8.
[4] E. Raub, G. Dehoust and E. Ramcke, *Metall.* **22** (1968) 573.
[5] L. Domnikov, *Metal Finish.* February (1966) 66.
[6] US Patent 3 219 558 (1965).
[7] German Patent 1 181 025 (1967).
[8] German Patent 1 235 103 (1970).
[9] German Patent 1 240 715 (1970).
[10] German Patent 1 246 349 (1972)
[11] USSR Patent 287 482 (1971).
[12] Bulgarian Patent 21 747 (1975).
[13] USSR Patent 2 651 041 (1980).
[14] Bulgarian Patent 54 726 (1981).
[15] E. Grünwald and C. Varhelyi, *Galvanotechnik* **70** (1979) 437.
[16] S. H. Finkelstein, L. N. Vizgalova, G. A. Vartanova and J. I. Surov, *Zashch. Met.* **16** (1980) 639.
[17] USSR Patent 2 659 324 (1980).
[18] Bulgarian Patent 54 956 (1982).
[19] P. M. Vjacheslavov, S. J. Griliches, G. K. Burkat and E. G. Kruglova, 'Galvanotechnika blagorodnih i redkih metallov', Mashinostroenie, Leningrad (1970) p. 48.
[20] German Patent 2 650 030 (1977).
[21] US Patent 4 246 077 (1981).
[22] I. Kristev and M. Nikolova, *J. Appl. Electrochem.* **16** (1986) 703.
[23] V. E. Dauiotis, G. A. Baltrunas and V. A. Kaikaris, *Elektrokhimiya* **19** (1983) 264 (in Russian).
[24] M. R. Collonguess in Nouveau Traite de Chimie Minerale sous la Direction de Paul Pascal, Deuxieme Fasciculu, Masson et C^{IE}, Paris, T. XX, (1963) p. 1014.
[25] N. P. Fedotjev and P. M. Vjacheslovov, *Plating* July (1970) 700.